ELSEVIER

Polymer 44 (2003) 3071–3083

polymer

www.elsevier.com/locate/polymer

Effect of penetrant size, shape, and chemical nature on its transport through a thermoset adhesive. II. Esters

Kermit S. Kwan[a], Chitra N.P. Subramaniam[b], Thomas C. Ward[b,*]

[a]Department of Materials Engineering and Science, Virginia Polytechnic Institute and State University, Blacksburg, VA 24061, USA
[b]Department of Chemistry, Virginia Polytechnic Institute and State University, 2107 Hahn Hall, Blacksburg, VA 24061, USA

Received 22 August 2002; received in revised form 31 January 2003; accepted 5 February 2003

Abstract

The transport properties of a series of ester penetrants through a polyamide-based elastomeric adhesive are reported. The results obtained are compared with those from a similar study on a series of *n*-alkane penetrants reported previously. It was established that the diffusion of the esters, as in the case of *n*-alkanes, is Fickian and follows a Henry's law-type mechanism. Furthermore, it was concluded from a combination of activation energy calculations and molecular simulations that the ester penetrants, similar to *n*-alkanes, diffuse linearly along their long molecular axes. The chemical composition influence of the penetrants was investigated by means of their Flory–Huggins interaction parameter with the elastomer, χ_{12}. The χ_{12} values for the esters were found to be lower than those of the corresponding *n*-alkanes suggesting the role of favorable contributions from the polymer–ester interactions. Differences in the diffusion coefficients between the *n*-alkane and ester series were explained on the basis of these χ_{12} values. Finally, correlations between (a) the diffusion parameters, D and E_d, (b) penetrant size (molar volume, V_m) and (c) chemical nature of the penetrant (χ) were established. These correlations account for both penetrant size and chemical effects simultaneously, thereby providing a more general description of the transport properties of the polymer–*n*-alkane and polymer–ester systems.

Keywords: Transport; Diffusion; Esters

1. Introduction

The transport properties of a series of *n*-alkane penetrants ranging from hexane (HX) (C_6) to heptadecane (HPD) (C_{17}) through a polyamide-type elastomeric matrix have been studied in detail, and the results were presented in a previous publication [1]. Since the *n*-alkanes displayed negligible specific interactions with the polymer matrix, these early experiments enabled an isolation of the effects of penetrant size and shape on the transport properties, without interference from polymer–penetrant energetics. It has been reported [2,3], however, that the presence of specific interactions between a penetrant and a polymer matrix can have a significant influence on the resulting transport behavior. Recent studies on the diffusion of organic esters through a fluoroelastomer membrane [2,3] have demonstrated the predominance of intermolecular forces. In those publications, with increasing molecular weight of the esters and/or the number of ester functionalities, the diffusivity was found to depend more on the chemical nature than on the molecular size of the penetrant. Another publication that highlights the effects of the chemical composition of the penetrants presents a study of the diffusion behaviors of linear alkanes, linear alcohols and substituted phenols in polyolefins [4]. The alkanes were found to follow the expected behavior based on molecular weight, while the alcohols and substituted phenols exhibited lower diffusion coefficients than the corresponding alkanes due to their tendency for penetrant clustering. However, as the number of carbon atoms increased, both the alcohols and phenols were found to approach the behavior of the alkanes as a result of increased shielding of the hydroxyl group. From these results, the authors [4] concluded that linear alkanes diffusivities could be considered as defining an upper limit for the transport behavior of polar, alcohol penetrants. Similar observations were also made in a study on the

---

[*] Corresponding author. Tel.: +1-540-231-5876; fax: +1-540-231-8517. *E-mail address:* tward@vt.edu (T.C. Ward).

0032-3861/03/$ - see front matter © 2003 Elsevier Science Ltd. All rights reserved.
doi:10.1016/S0032-3861(03)00158-7

diffusion of hindered phenols in low density polyethylene by Möller and Gevert [5].

The above mentioned investigations have considered the transport of polar penetrants through an essentially non-polar polymer matrix. Systems involving a polar or reactive polymer (in addition to a polar penetrant) can introduce additional chemical effects that strongly influence diffusion behavior. Aminabhavi and Khinnavar [6] have carried out a study on the diffusion of aliphatic alcohols in a variety of polymers including polyurethanes, nitrile-butadiene rubbers and epichlorohydrin membranes. These authors have demonstrated significant impact on the transport behavior from the polarity of the penetrant, which was compounded by an increased hydrogen bonding ability of the polymers.

The present study was initiated to further our understanding of the role of molecular structure on the polymer–penetrant interactions controlling the resulting transport behavior of a model system. This has been achieved by investigating the transport of a series of ester penetrants into an elastomeric polyamide-type matrix. The polymer matrix used was the same as in the previous *n*-alkane report [1] so that a direct comparison of the results obtained from the two types of penetrants, i.e. *n*-alkanes and esters, could be achieved. Such a comparison is detailed below and provides further insight into the variations in diffusion caused solely by differences in chemical nature (polarity) of one of the components. Furthermore, correlations between the diffusion parameters and the size and chemical nature of the penetrants have been developed, and are discussed at length in this paper. All of this data provide the basis for integration into the third paper of this sequence which unites the model to include mechanical behavioral changes.

2. Experimental

A homologous series of esters ranging from methyl acetate, MA (C_3) to isopropyl myristate, IPM (C_{17}), plus another ester, isodecyl pelargonate, IDP (C_{17}), was used as the penetrants in the present study. IDP is an isomer of IPM (C_{17}), and was included in order to determine the influence of the relocation of the ester moiety on the transport behavior. IDP (Emery 2911) was obtained from Emery Chemicals (99.9 + %). All other materials (99.9 + % purity) were purchased from Aldrich Chemical Co™. The molecular weights, molar volumes, and solubility parameters for all the above molecules are listed in Table 1. The range of molecular weights of the ester penetrants were selected to resemble that of the *n*-alkane series discussed in the previous publication [1], thereby allowing a direct comparison of the two types of species.

As mentioned earlier, the same polyamide-type polymer matrix used in the previous investigation on *n*-alkanes [1] was also used in the present research. This polymer was cured at 100 °C for 1 h followed by a post-cure at 150 °C for 3 h. Rectangular pieces ($2.54 \times 1.27 \times 0.05$ cm^3) of cured polymer were cut from the cured polymer film for solvent uptake measurements. These measurements for the polymer–ester systems were carried out as a function of time at test temperatures of 23, 45, 55, 65 and 85 °C, using an analytical balance as described previously [1].

The glass transition temperatures (T_g) of the polymer samples saturated with the different ester penetrants were determined by means of differential scanning calorimetry (DSC). Broad glass transition regions with the onset temperatures ranging from -25 to 20 °C were obtained, thereby indicating that the polymer is in the rubbery state at all the test temperatures examined in this work.

The modulus of the polymer was determined from its stress–strain behavior using an Instron™ 5500R Materials Tester in conjunction with an extensiometer and an Instron™ model 3116 furnace attachment. The load cell had a 200 lb maximum and samples were held in place using two pneumatic clamps. Samples 0.02 in. thick were cut using an ASTM Type IV D638 die whose gauge length and width were 10 and 0.25 in., respectively. The stress–strain behavior was measured using five test specimens. The samples were held at 150 °C for 15 min prior to testing at that same temperature. A crosshead speed of 10 mm/min was used for all experiments and the samples were stretched to 40% elongation. Stress relaxation was allowed to occur until an equilibrium stress was reached (ca. 25 min). Equilibrium engineering stress (σ) and strain (ε) values for the samples were used to calculate their moduli and molecular weights between crosslinks (M_c) based upon the theory of rubber elasticity, as outlined in Appendix A. The equilibrium modulus values were calculated for the five samples tested and the average values are reported.

Polymer density at room temperature (~23 °C) was determined using a Micromeritics™ Accupyc 1330 gas displacement pycnometer (0.002% error). The polymer samples were weighed using a Denver Instruments™ Microbalance, and then placed in the pycnometer sample cup of volume equal to 1 cm^3. Then, the sample enclosure was purged with He gas and measurements for the volume and density of the sample were obtained. This process was repeated five times for each sample, and the polymer density (ρ_p) at 23 °C was determined from the average values collected from three test specimens (a total of 15 measurements).

The polymer densities at different temperatures were determined using a technique based upon optical microscopy. A polymer sample was placed into an Olympus™ BH-2 optical microscope with a Linkam™ THM 600 hot stage. Samples were heated and held isothermally at various test temperatures (20–170 °C in 5–10 °C increments) for at least 10 min to reach thermal equilibrium. Olympus™ CUE Micro300 video calipers (± 0.001 μm) were used to measure the changes in the *x* and *y* dimensions of the samples. Data was collected during both heating and cooling cycles, in order to check for repeatability of the measurements. The linear expansions of

Table 1
Properties of ester penetrants

Penetrant	Molecular weight (g/mol)	Molar volume (cm^3/mol)	Solubility parameter ($MPa^{0.5}$)
Methyl acetate (MA)	74.07	79.86	19.4
Ethyl propionate (EP)	102.12	115.45	17.9
Propyl butyrate (PB)	130.19	149.97	17.2
Ethyl heptanoate (EH)	158.24	183.09	17.0
Ethyl nonanoate (EN)	186.30	216.24	16.9
Ethyl undecanoate[a] (EU)	214.35	249.53	16.7
Ethyl myristate[a] (EM)	256.43	299.22	16.6
Isodecyl myristate[a] (IPM)	270.46	318.19	16.5
Isodecyl pelargonate[a] (IDP)	270.46	314.56	16.4

[a] Calculated using Hansen's method.

the samples as determined earlier were converted into volume expansions, assuming isotropic behavior. The polymer densities at the different temperatures were estimated from the volume expansion values, in conjunction with the density of the polymer at 23 °C (from pycnometry).

3. Results and discussion

The mass uptake with time, t, of many polymer–penetrant systems has been shown [7,8] to follow a power law expression of the form,

$$\frac{M_t}{M_\infty} = Kt^n \tag{1}$$

where M_t and M_∞ are the experimental mass uptakes at time t and ∞, respectively, K is a constant dependent upon the structural characteristics of the polymer and the solvent, and n is an exponent related to the transport mechanism, as follows [2,3,7,8,9]: $n = 0.5 \Rightarrow$ Fickian transport, $n = 1.0 \Rightarrow$ Case II transport, and $0.5 < n < 1.0 \Rightarrow$ anomalous transport.

It was demonstrated in the previous publication [1] that the diffusion of linear n-alkane penetrants through the polyamide-type polymer matrix follows this expression (Eq. (1)) and is Fickian ($n \cong 0.5$). The sorption data obtained for the esters of the present study was also analyzed based upon Eq. (1). Non-linear curve fitting of the fractional mass uptake, M_t/M_∞ of the ester data was executed up to 97% of the equilibrium value and the K and n values evaluated. As in the case of n-alkanes, all the ester penetrants exhibited n values close to 0.5, typical of ideal Fickian diffusion [6]. This behavior is a consequence of rapid segmental motions in the polymer matrix (due to its low T_g) that minimize relaxation effects [3]. The values of K exhibit a systematic increase with decreasing number of carbon atoms and with increasing temperature. The temperature dependence of K is attributed to both an increase in mobility and in the free volume within the polymer with increasing temperature. The inverse dependence of K on penetrant molecular weight is a direct reflection of the decreasing solubility associated with larger penetrants.

The Fickian nature of the sorption data for the polymer–ester systems was further verified from the reduced sorption plots, i.e. plots of M_t/M_∞ versus $t^{0.5}$ (normalized by film thickness). One such plot for the ester penetrants at 23 °C is shown in Fig. 1. Curves of similar shape were obtained at the different test temperatures. As in the case of n-alkanes [1], these curves are found to possess the Fickian characteristic of linearity up to 60% mass uptake ($M_t/M_\infty = 0.60$).

Having verified the Fickian nature of the transport process, diffusion coefficients, D, were calculated using a 'thin-film' solution for the Fickian model. The boundary conditions for this case were outlined in the previous publication [1]. We recall that D is related to the initial slope [10] of the reduced sorption curves as $D = \pi/4\ (\text{slope})^2$. Accordingly, values of D for the esters were calculated at the different test temperatures, and are listed in Table 2. It is seen from the table that the values of D exhibit a steady increase with decreasing molecular weight of the penetrants and with increasing temperature. These observations are similar to those made on the n-alkanes as well as to those from a number of other previous investigations on similar diffusants, and may be explained based upon free volume arguments [6,11–15]. This increasing trend in D with decreasing molecular weight of the esters further indicates the absence of penetrant clustering. If present, clustering

Table 2
Diffusion coefficients, D ($\times 10^9$ cm^2/s) for the ester penetrants at different test temperatures

Penetrant	Temperature (°C)				
	23	45	55	65	85
Methyl acetate	40.5	148	215	300	–[a]
Ethyl propionate	26.0	70.1	132	182	370
Propyl butyrate	10.3	39.4	61.7	93.9	198
Ethyl heptanoate	5.77	24.0	40.8	64.9	125
Ethyl nonanoate	2.48	12.8	21.1	33.9	68.6
Ethyl undecanoate	1.40	7.79	12.5	18.6	49.2
Ethyl myristate	391	3.07	6.46	8.46	34.6
Isopropyl myristate	0.216	1.67	3.85	5.73	21.5
Isodecyl pelargonate	0.0516	0.496	1.71	2.76	11.6

[a] Data not obtained due to its low boiling point.

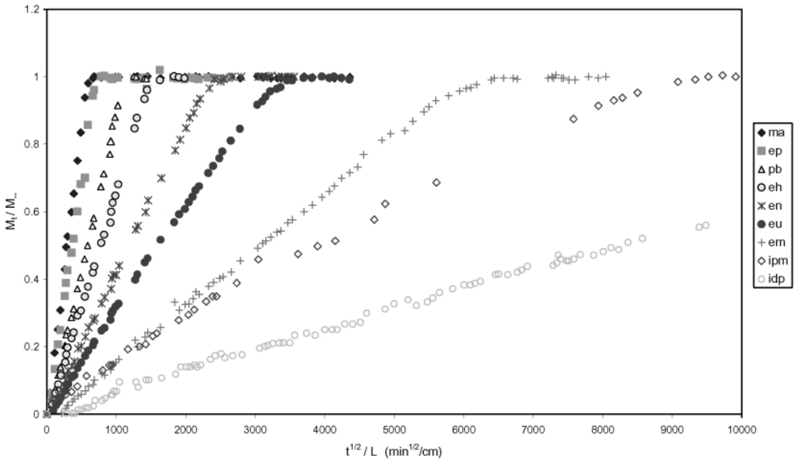

Fig. 1. Reduced sorption plots for ester penetrants at $T = 23$ °C. Legend tags are in Table 1.

would result in lower diffusion coefficients for the lower molecular weight esters [4] in accordance with their higher solubility parameters listed in Table 1.

The dependence of the diffusion coefficients (diffusivity) upon penetrant size has been previously [16–18] described by a power law expression, given by

$$D = bM^a \tag{2}$$

where D is the diffusivity (cm^2/s), M is the molecular weight of penetrant (g/mol), and b and a are material parameters.

As suggested by Eq. (2), the experimental D values obtained at different test temperatures for the esters were plotted as a function of penetrant molecular weight, M. The results at a given temperature were fit using a Levenburg–Marquedt algorithm. Poor agreement between Eq. (2) and the data was observed indicating that the power law expression does not adequately describe the molecular weight dependence of the diffusivity of these penetrants. Earlier we found that excellent fits were achieved with this expression when *n*-alkanes were the mobile molecules penetrating the same polymer matrix [1]. The inability of Eq. (2) to accurately describe the D versus M relationship for the esters is further exemplified from plots of log D versus log M for these penetrants as shown in Fig. 2. The corresponding data for *n*-alkanes are included here for comparison. For purposes of clarity, only two test temperatures for each penetrant type are represented. It is clear from the figure that the *n*-alkanes exhibit a linear dependence over the entire molecular weight range studied. However, the esters' data display a significant curvature with the extremes approaching the behavior of the *n*-alkanes. This behavior is directly related to the polar nature of the esters that results in significant polymer–penetrant interactions in contrast to the non-polar *n*-alkanes having negligible interactions with the polymer matrix. The fact that the larger esters approach the behavior of the corresponding *n*-alkanes is indicative of overall weaker interactions of these larger molecules per unit mass with the polymer, mainly as a result of 'dilution' of their polarity with the increasingly longer non-polar segments. The diffusion coefficients for the lowest molecular weight esters (MA and ethyl propionate (EP)) are approaching the behavior exhibited by the *n*-alkanes which could imply that these molecules may be below the critical molar volume beyond which chemical nature of the penetrant molecules becomes significant. In this case of MA and EP, the diffusivities may be dictated to a larger extent by the large mismatch of smaller diffusant molar volume with larger fluctuating hole size of the matrix rather than its chemical nature. Furthermore, the diffusion coefficient for EP may be viewed as representing a transition where the chemical effects on D begin to become less significant (while moving towards lower penetrant masses).

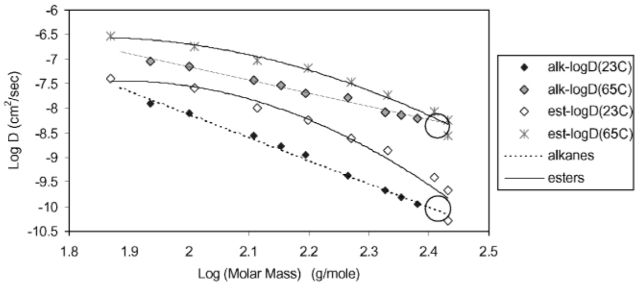

Fig. 2. Variation of diffusion coefficient as a function of molar mass for the *n*-alkanes and the esters homologous series at 23 and 65 °C.

The deviation from a linear behavior (curvature) for the ester series data seen in Fig. 2 represents a failure of the power law expression in describing the transport behavior of these penetrants. The inadequacy of this expression in describing other polar systems such as phenolic penetrants has been demonstrated by other investigators [5]. It is known that Eq. (2) has an implicit assumption that the molar mass is the dominant factor in determining transport behavior, without regard to penetrant shape and chemical nature. Hence, the above discussion suggests that factors other than molecular mass must play a significant role in determining the diffusion properties of our esters. Thus, factors such as shape and chemical nature of the molecules need to be evaluated in a suitable model. Therefore, it is clear that a better description of the transport properties of the ester penetrants, encompassing the effects of all the factors discussed earlier, is necessary and is presented below.

We turn now to the thermodynamics and kinetics of the diffusion. It may be seen from Table 2 that the diffusion coefficients, D, increase with temperature, T, for a given penetrant. The temperature dependence of the diffusion coefficients was analyzed based on the Arrhenius equation,

$$D = D_0 \exp\left(\frac{-E_\mathrm{d}}{RT}\right) \tag{3}$$

where E_d is the activation energy of diffusion (kJ/mol), D_0 is the Arrhenius front factor, and R is the gas constant.

Graphs of log D versus $1/T$ were constructed for all the polymer–ester combinations studied. Values of E_d and D_0 were determined from the slopes and intercepts of these plots, respectively. The E_d values are plotted as a function of molar mass in Fig. 3, and are found to increase with increasing penetrant size suggesting that more complex segmental motions may be necessary for the diffusion of the larger molecules [9,19]. It is also noted that the E_d values for the esters are of the same order of magnitude as those estimated for the *n*-alkanes reported in the previous publication [1] and are typical of diffusion into a rubbery matrix [20]. Such a comparison of the esters and the *n*-alkanes is also depicted in Fig. 3.

The activation energies for the lowest molecular weight penetrants of the esters and alkanes coincide. E_d for the remaining esters are generally lower than those of the corresponding alkanes. The lower E_d values for the esters may be attributed to the polar ester functionality that could result in favorable polymer–penetrant interactions, thereby enhancing the ease of diffusion of the ester penetrants. This aspect of the chemical nature of the penetrants is discussed in greater detail in Section 3.2. The behavior observed in the lower molecular weight data region in Fig. 3 (alkanes and esters asymptote with an E_d of approximately 42 kJ/mol) could be related to a critical penetrant size below which only molecular volume dominates diffusion with the effect due to the polar ester group remaining negligible. Thus, E_d becomes independent of chemical type since normal, segmental motions resulting from thermal energy are sufficient to allow the penetrant molecules to diffuse in a simple 'step'. For larger molecules, however, the E_d values of both series begin to increase with penetrant size with the alkanes exhibiting a stronger variation than the ester series. This result may be related to the favorable polymer–penetrant interactions discussed earlier.

It is also noted from Fig. 3 that the E_d value for IDP is considerably higher than that for IPM although the two molecules are characterized by identical molar masses. We note that IDP and IPM are isomers, with the ester moiety located in the middle of the IDP molecule in contrast to attachment near the end of IPM. This effect of the isomerism on penetrant shape, and in turn on the resulting transport behaviors, is discussed in Section 3.1.

The linear correlation between the Arrhenius terms, E_d and log D_0 (Eq. (3)), has been experimentally demonstrated for a number of polymers [5,16,21–25]. This relationship for the ester penetrants of the present investigation is verified by plotting log D_0 versus E_d as shown in Fig. 4. The data for the *n*-alkane systems from our previous study [1] are also included for comparison. It is found that both series of data can be represented by a single straight line of slope 0.113. Furthermore, this slope is in excellent agreement with the literature value of 0.10 for elastomeric materials reported by van Krevelen [26].

The correlations established above between penetrant size and E_d, and between E_d and D_0 can now be used to predict diffusion coefficients for penetrant molecules similar to both *n*-alkanes and esters using the general form of the Arrhenius equation [19,26]. This scheme involves:

(1) Extrapolating the activation energy, E_d from knowledge of molecular size of the penetrant (using Fig. 3)
(2) Determining corresponding D_0 from its dependence on E_d (via Fig. 4), and
(3) Substituting the E_d and D_0 values from steps 1 and 2 above into Eq. (3), to determine the diffusion

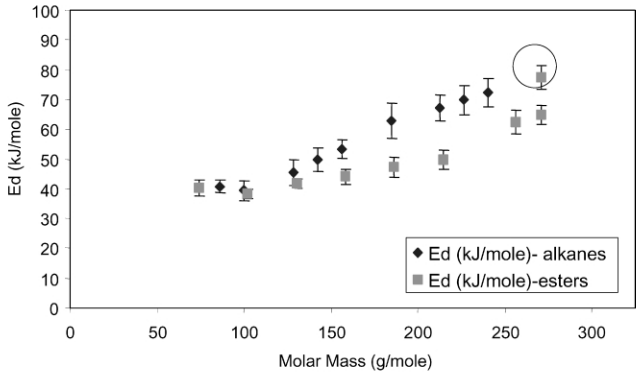

Fig. 3. Activation energies of diffusion, E_d, as a function of molar mass for the *n*-alkane and ester penetrants.

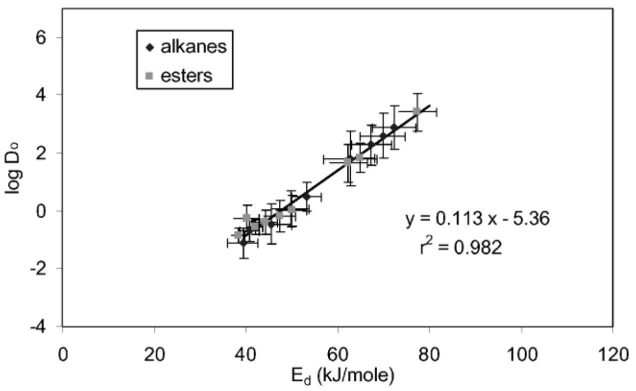

Fig. 4. Relationship between the Arrhenius parameters, D_0 and E_d for *n*-alkane and ester penetrants in the rubbery matrix.

coefficient, D for the polymer–penetrant system at a given temperature, T.

Further insight into the mechanism of ester sorption was gained by considering the equilibrium sorption values (i.e. solubilities) for the polymer–ester systems. Equilibrium sorption may be defined as the equilibrium mass of penetrant absorbed per gram of polymer, i.e. $M_\infty/M_{t=0}$. These values were directly calculated from the diffusion data acquired for the polymer–ester systems and are listed in Table 3. As in the case of *n*-alkanes [1], the solubilities for the esters increased with decreasing penetrant size. However, the esters display higher solubilities than the corresponding alkanes. These observations can be associated with a combination of entropic and enthalpic factors that result in a lower free energy of mixing for the polymer–ester series. In other words, decreasing the penetrant size increases ΔS_{mix}, thereby favoring mixing. In addition the polarity of the smaller ester penetrants are relatively high due to the fact that the ester group comprises the majority of the volume of the molecule. This enhances the potential for specific interactions with the polyamide-type polymeric matrix (more negative ΔH_{mix}). With an increase in the number of carbon atoms, however, the polarity of the penetrant molecule is 'diluted' by the addition of a longer hydrophobic methylene sequence whose flexibility permits the molecule to 'fold' back on itself, and thus shield the ester functionality.

The equilibrium sorption values discussed earlier may also be regarded as thermodynamic equilibrium sorption constants designated as K_s. This constant is related to the thermodynamic enthalpy (ΔH_0) and entropy (ΔS_0) by means of the van't Hoff equation,

$$\text{Log } K_s = \frac{\Delta S_0}{2.303R} - \frac{\Delta H_0}{2.303RT} \tag{4}$$

Based on this equation, plots of log K_s versus $1/T$ for all the polymer–ester data were constructed. The ΔH_0 and ΔS_0 values were evaluated from the slope and intercept of these plots, respectively, and are listed in Table 4. It is seen from the table that the ΔS_0 values become increasingly negative with increasing penetrant size. This result is similar to that obtained for the *n*-alkanes [1] and can be explained based on the neighboring polymer chains being compressed to a greater extent in order to accommodate the larger penetrants, thereby increasing the overall order of the matrix (i.e. a more negative ΔS_0) [7,10]. As discussed previously [1], the ΔH_0 parameter contains information reflecting the type of sorption mechanism (e.g. Henry's law, Langmuir-type, etc.). The Henry's law mechanism involves an endothermic process ($\Delta H_0 =$ positive) resulting in the formation of a vacant site, followed by filling of that site by a penetrant molecule. The ΔH_0 values for all the esters were positive (~10 times greater than for *n*-alkanes), thereby suggesting that a Henry's law-type of mechanism is involved in the sorption process. It has been demonstrated in the previous study [1] that the same Henry's law mechanism is also followed during the sorption and passage of *n*-alkane penetrants through the polymer matrix. In addition, as in the case of the *n*-alkanes [1], it was also established in this present study that the experimental diffusion data for the esters follow the first order kinetic equation [27–31].

Table 3
Equilibrium sorption values (% mass uptake) for esters at different test temperatures

Penetrant	Temperature (°C)				
	23	45	55	65	85
Methyl acetate	16.5	20.3	22.2	24.7	–[a]
Ethyl propionate	18.3	20.7	23.5	25.3	26.5
Propyl butyrate	16.9	20.6	21.2	22.9	23.9
Ethyl heptanoate	15.0	18.1	18.2	19.9	20.4
Ethyl nonanoate	12.1	14.8	15.0	16.4	15.7
Ethyl undecanoate	10.7	12.8	12.8	13.9	13.8
Ethyl myristate	7.69	9.01	8.93	9.62	10.1
Isopropyl myristate	6.67	7.48	7.32	7.85	8.18
Isodecyl pelargonate	6.28	6.91	6.86	7.35	7.83

[a] Data not obtained due to its low boiling point.

Table 4
Enthalpy, ΔH_0 (kJ/mol) and entropy of sorption, ΔS_0 ($\times 10^2$ kJ/mol/K)

Penetrants	ΔH_0	ΔS_0
Methyl acetate	7.82	11.4
Ethyl propionate	5.64	4.95
Propyl butyrate	4.97	2.23
Ethyl heptanoate	4.53	−0.27
Ethyl nonanoate	3.95	−3.84
Ethyl undecanoate	3.77	−5.61
Ethyl myristate	3.88	−8.10
Isopropyl myristate	2.85	−12.6
Isodecyl pelargonate	3.08	−12.8

At this point in the discussion, it has been shown that the transport of the ester penetrants into the polymer matrix is Fickian and that it proceeds via a Henry's law-type mechanism. Furthermore, the effects of penetrant size on the diffusion parameters such as D and E_d have been quantified. The results obtained were also compared to the transport of *n*-alkanes through the same polymer matrix. In contrasting the two series of penetrants, it was obvious that factors in addition to penetrant molecular weight (volume) play a significant role in determining the transport behavior of the esters. The deviations observed between the two series of penetrants were associated with the presence of the polar ester functionality. Unlike the simple case of the *n*-alkanes, the polar ester moiety can greatly alter the penetrant shape as well as result in significant specific interactions between the polymer matrix and the small molecule. Therefore, the influence of the *shape* and *chemical nature* of the ester penetrants on their final transport behavior has been investigated in depth and the results are discussed below.

3.1. Effect of shape

The diffusion of small molecules such as simple gases and lower molecular weight organic molecules (<6 carbon atoms) may be described by assuming a spherical geometry for the penetrant. Such molecules can diffuse through a polymer matrix without requiring major re-arrangement of the polymer chain segments. However, in the case of larger penetrants, spherical geometries may not be applicable since even greater redistribution of the polymer chains would be required to accommodate a large sphere as opposed to a cylinder, etc. As a result, such a molecule would assume a shape that would minimize its space requirements. This shape is determined by the free energy conformation minima that are available to the molecule and the polymer. It has been demonstrated via sorption studies [5,15,18,32] that the transport of esters within a matrix favors an extended geometry that results in the least perturbation of the polymer chains. It has also been reported [13,14] that a similar geometry is preferred in the self-diffusion of low molecular weight liquids as well as at different concentrations within a polymer matrix. In the present investigation on ester penetrants, the penetrant geometry during diffusion has been determined using activation energy calculations and Monte–Carlo simulations.

The activation energy calculations involved the estimation of E_d/CH_2 values for the penetrants, as listed in Table 5. These calculations are based on previous literature [5,32] that indicate that increasing the number of CH_2 units only lengthens the molecule without altering its diffusion diameter. The E_d/CH_2 values (from Table 5) for all the esters, except IDP, are found to be consistent with the reported [5] range of 1–3.5 kJ/mol for the diffusion of esters parallel to the long molecular axis.

It is also noted from the table that the difference between the E_d values of MA (C_3) and EP (C_5) is negligible. It may be speculated that these two penetrants are below a molecular size beyond which shape effects become significant. Another case in which the shape effects may play a major role is that of the penetrant IDP, whose E_d/CH_2 value is inconsistent with diffusion along the major axis. The transport of this molecule will be discussed in detail in Section 3.2.

Table 5
Activation energy per addition of a methylene (CH_2) unit (kJ/mol/CH_2) for the ester penetrants

Esters	
Number of carbons	E_d/CH_2-unit
5	0
7	1.85
9	1.11
11	1.59
13	1.27
16	4.14
17	2.45
17[a]	15.08

[a] Isodecyl pelargonate (IDP).

Further information on the shape of the ester penetrants was obtained from a series of Monte–Carlo simulations using Macromodel® 5.0. Specific details regarding the experiments and analysis have been described in the previous publication [1], and a complete description is also available in the original work [33] related to this paper. The aspect ratios (defined as length/diameter, $L/2r$) of the ester penetrants were evaluated from the simulations and are listed in Table 6. The ratios for the *n*-alkanes from the previous paper [1] are also included in this table for comparison. It was found that the aspect ratios for both series of penetrants increase with increasing number of carbon atoms, displaying larger deviations from an $L/2r$ value equal to one (sphere). However, a small decrease in aspect ratios is observed for the penetrants with $C > 15$, suggesting the greater probability of the longer hydrocarbon segments to fold. This folding behavior is facilitated by the high degree of flexibility possessed by the methylene moieties that comprise the hydrophobic tails of these molecules. The fact that both the *n*-alkanes and esters exhibit similar values and trends with respect to shape is probably related to the location of the ester functionality near the end of the ester molecule. As a result, the methylene sequence of the esters acts essentially independent of the ester moiety, behaving more like the *n*-alkanes. This is particularly significant for penetrants with $C > 6$.

The lower molecular weight members of both series (HX and EP) display aspect ratios approaching a value of 1 due to their shorter lengths. Furthermore, it was demonstrated from the E_d/CH_2-unit calculations that the difference between HX and heptane (HP), and between MA and EP was negligible. It may be inferred from this result that the aspect ratios of these four penetrants may also be comparable. It is also clear from Fig. 3 that the activation energies for the four penetrants—HX, HP, MA, and EP-coincide. Thus, the transport mechanisms of these four species must be similar, in spite of differences in their chemical types and molecular weights. At the same time, considerable differences in the E_d values between the higher molecular weight esters and *n*-alkanes can be seen in Fig. 3. Therefore, it may be concluded that the HX, HP, MA, and EP molecules are below a critical size above which the effects of the chemical nature of the penetrants become significant. Another conclusion that may be drawn from this discussion relates to the actual steps involved in the diffusion process of the four penetrants: HX, HP, MA and EP. While having similar aspect ratios (close to 1) and activation energies of diffusion, but different molecular weights, their diffusion is dominated by a more elemental translation step.

Thus, it is now clear that the differences observed in the diffusion behaviors of the esters and *n*-alkanes are not a result of differences in their shapes. One exception to this

Table 6
Geometrical parameters obtained from Monte–Carlo simulations of *n*-alkane and ester penetrants (length/diameter = $L/2r$)

Penetrant	Volume (Å^3)	Average radius (Å)	Average cross-section area (Å^2)	Average aspect ratio ($L/2r$)
Ethyl propionate (C_5)	109.0	2.198	15.19	1.636
Ethyl heptanoate (C_9)	179.0	2.459	19.21	2.050
Ethyl nonanoate (C_{11})	213.5	2.482	19.61	2.399
Ethyl myristate (C_{16})	299.5	2.598	21.69	3.069
Isopropyl myristate (C_{17})	318.0	2.696	23.27	2.889
Isodecyl pelargonate (C_{17})	318.0	3.270	33.66	1.467
Hexane (C_6)	113.6	2.354	17.46	1.409
Nonane (C_9)	167.5	2.292	16.53	2.238
Decane (C_{10})	186.0	2.296	16.60	2.478
Tridecane (C_{13})	239.5	2.390	18.14	2.948
Pentadecane (C_{15})	270.5	2.450	19.16	3.163
Hexadecane (C_{16})	291.0	2.639	22.20	2.750
Heptadecane (C_{17})	308.5	2.708	23.48	2.780

conclusion, however, is IDP whose transport properties differ from the rest of the esters as well as from the *n*-alkanes. The possible reasons leading to this behavior are discussed below.

IDP was included in the present study in order to understand the effect of the placement of the ester functionality on the resulting transport behavior. In IDP, the ester group is located in the middle of the molecule in contrast to the rest of the esters where the ester functionality is positioned near the end. This difference is seen to greatly influences the transport properties of IDP. We analyze this by noting the aspect ratio for IDP (Table 6) is much lower than that of other penetrants (IPM, HPD) with the same number of carbon atoms (C_{17}). The lower aspect ratio can be attributed to the bond angles about the ester group in IDP that allow its aliphatic tail to coil, thereby tending towards a more sphere-like geometry. The corresponding increase in diffusion cross-section is consistent with the abnormally large E_d/CH_2 value estimated for IDP (Table 5). This large area also makes it more difficult for the polymer matrix to accommodate this penetrant molecule. Similar results have also been reported from other studies on the self-diffusion of trace combinations of ester plasticizers in rubbery PVC [14,34]. These results indicate that the self-diffusion coefficient decreases by a factor of 3 per additional Angstrom of the streamlined cross-section of the plasticizer. Furthermore, the ester group in IDP is more shielded, thereby eliminating some of the favorable polymer–penetrant interactions that may have occurred. The above explanation is consistent with the ‘shielding’ behavior that has been observed in phenolic alcohols [4] as a result of the presence of an aliphatic branch adjacent to the OH group.

The concepts discussed earlier are also reflected in the unique behavior of IDP observed in Figs. 2 and 3 (as indicated by the circles). The lower diffusion coefficient and higher activation energy for IDP relative to IPM are a direct consequence of the placement of the ester moiety in the middle of the IDP molecule.

3.2. Effect of chemical nature

The origin of describing the transport behaviors of penetrants in terms of their chemical nature dates back to the early studies by Koszinowski [21] and Eyring [35]. These authors observed that diffusivity and activation energy of diffusion could be related to the heats of vaporization of the penetrants. The chemical nature of penetrants can be described in terms of a solubility parameter (δ) that is a material property of the pure penetrant and is readily available from the literature. Although the use of this parameter is attractive in terms of ease of use, it does not describe the extent of specific interactions between a polymer–penetrant pair. A better description of the chemical nature of a system is provided [36,37] by the Flory–Huggins interaction parameter (χ), χ_{12}. Although the values of χ_{12} for commonly used polymer–penetrant systems are available in the literature, the χ_{12} values for the polymer–penetrant pairs in the present study are not. These χ_{12}s therefore need to be experimentally determined. This has been done by first evaluating the molecular weight between crosslinks, M_c, of the polymer matrix, based on the theories of rubber elasticity [38,39]. Then, the M_c value in conjunction with the experimental mass uptake data for both penetrant series, was analyzed using the Frenkel–Flory–Rehner (FFR) swelling theory to yield effective chi values (χ_{12}) for all the systems studied at all of the test temperatures. Further details of these calculations and the assumptions involved in the FFR hypothesis are outlined in Appendix A. The χ_{12} values thus estimated for the *n*-alkane and the ester penetrants are listed in Tables 7 and 8, respectively. These experimentally determined ‘effective’ χ values are higher than would be expected for an uncrosslinked polymer in a solvent. This deviation could be a result of the crosslinked nature of the polymer in the present study, which introduces some uncertainty in the chemical

Table 7
Evaluated χ_{12} parameters for *n*-alkane penetrants at the different test temperatures

Penetrant	Temperature (°C)				
	23	45	55	65	85
Hexane	1.51	1.50	1.49	1.48	–[a]
Heptane	1.61	1.60	1.59	1.58	1.58
Nonane	1.76	1.70	1.69	1.69	1.70
Decane	1.81	1.76	1.75	1.75	1.77
Undecane	1.87	1.84	1.82	1.82	1.82
Tridecane	1.99	1.99	1.98	1.97	1.97
Pentadecane	2.17	2.15	2.13	2.12	2.10
Hexadecane	2.27	2.24	2.20	2.21	2.22
Heptadecane	2.31	2.31	2.25	2.29	2.28

[a] Data not obtained due to low boiling temperature.

structure, and/or deviations from the assumptions included in the FFR hypothesis. In spite of the variation, the effective χ_{12} values accurately mirror the trends in solubility observed from the experimental sorption curves. In other words, polymer–penetrant systems with a lower estimated χ_{12} value are characterized by higher experimental equilibrium sorption values.

It may be seen from Tables 7 and 8 that the χ_{12} values for the alkanes exhibit virtually no dependence upon temperature, indicative of low heats of solution. χ_{12} values for the esters, on the other hand, systematically decrease with increasing temperature, which indicates an increase in the 'energy' change associated with their sorption (with temperature). This behavior is consistent with the earlier discussion regarding the endothermic nature of the solution process for the esters. The difference in the temperature variation of the χ_{12} values between the two penetrant classes is most likely also related to differences in the chemical nature between the *n*-alkanes and esters. The aliphatic, non-directional intermolecular forces of the *n*-alkanes are more density dominated.

The effect of polymer–penetrant interactions on the transport behaviors of the penetrants may be further understood by considering the variation of the diffusion coefficients as a function of χ_{12}. A plot of log *D* versus χ for both series of penetrants (at 23 °C) is shown in Fig. 5. The molecular weights of all the penetrants are also indicated in the plot. Both the *n*-alkanes and esters are found to exhibit a steady increase in *D* with decreasing χ_{12} (stronger interactions). However, this result cannot be entirely attributed to increasingly favorable specific interactions in the polymer–penetrant systems since a decrease in penetrant molecular weights occurs in parallel with decreasing χ_{12} values. Therefore, the larger diffusion coefficients could be the combined result of the effects due to decreasing penetrant size and favorable specific interactions. In order to examine the influence of size, independent of chemical nature, it is useful to compare the diffusion coefficients of the two series at a selected χ_{12} value. Such a comparison shows that the diffusion of esters is slower (i.e. lower *D* value) than that of *n*-alkanes. This result can be associated to the larger size of the esters at a given χ_{12}. Likewise, the role of polymer–penetrant interactions can be studied independent of molecular size, by comparing the diffusion coefficients of the *n*-alkanes and esters with similar molecular weights (indicated by the straight lines in Fig. 5). It is found that the diffusivities of the esters are greater than those of the corresponding (molecular weight) alkanes. Clearly, this is a result of the presence of the polar ester group, leading to specific interactions in the polymer–penetrant system. Thus, in this case, the transport behavior is predominantly governed by the chemical nature of the ester penetrant.

Further information regarding the effects resulting from the contributions of the two parameters (size and chemical nature) for our polymer–penetrant systems may be obtained by considering the lowest molecular weight members of the ester series (Fig. 5). The log *D* versus χ_{12} curve for the esters exhibits a steady increase in *D* with decreasing χ_{12} and then increases sharply for the lowest molecular weight members, finally approaching the alkane plot. It is clear from the figure that EP and propyl butyrate (PB) display higher *D* values than the linear prediction. The greater diffusivities for these two molecules are the result of two favorable factors: (1) an increase in polarity, and (2) a decrease in molecular size. However, the case of MA is unique in that its experimental χ_{12} value is significantly higher (indicating weaker polymer–penetrant interactions) than that of the adjacent higher molecular weight ester species. Yet, the MA diffusion coefficient is much higher than the value expected if the straight-line trend in log *D* versus χ_{12} were followed. Therefore, it may be inferred that the higher *D* value obtained for MA is a result of the predominance of the favorable size effect. Further support for this statement is gained from the fact that the diffusion coefficient of MA approaches the curve for the *n*-alkanes. As noted earlier, the trend observed for the *n*-alkanes is a result of only the penetrant size effect, since it is known that polymer–penetrant interactions are negligible in this case.

Table 8
Evaluated χ_{12} parameters for ester penetrants at the different test temperatures

Penetrant	Temperature (°C)				
	23	45	55	65	85
Methyl acetate	1.37	1.25	1.21	1.15	–[a]
Ethyl propionate	1.29	1.21	1.15	1.12	1.09
Propyl butyrate	1.31	1.22	1.20	1.16	1.13
Ethyl heptanoate	1.38	1.27	1.27	1.22	1.20
Ethyl nonanoate	1.49	1.38	1.37	1.32	1.33
Ethyl undecanoate	1.57	1.45	1.45	1.40	1.40
Ethyl myristate	1.77	1.66	1.67	1.62	1.58
Isopropyl myristate	1.86	1.78	1.79	1.74	1.71
Isodecyl pelargonate	1.91	1.84	1.85	1.80	1.75

[a] Data not obtained due to low boiling point.

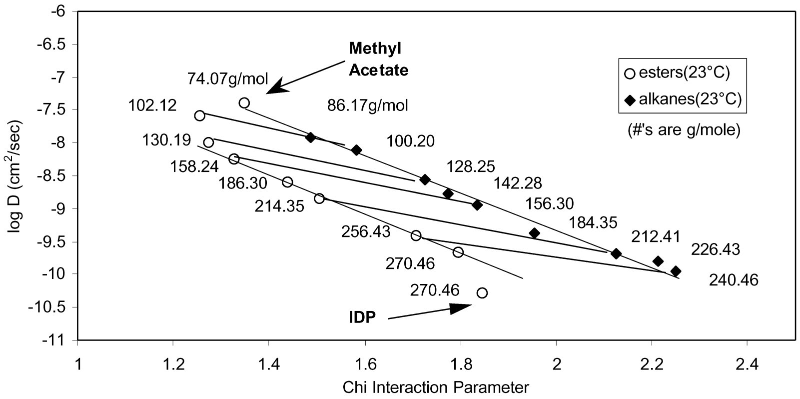

Fig. 5. Log diffusivity (cm^2/s) versus Flory–Huggins interaction parameter (χ) for *n*-alkanes and esters at 23 °C.

The effect of chemical nature of the penetrants discussed in the above paragraphs can now be used to explain the differences observed between the molar mass-dependence of the diffusion parameters, D and E_d, for the *n*-alkanes and esters. As discussed earlier, the diffusion coefficients, D for the esters (in Fig. 2) are larger than the corresponding molar mass alkanes. It was suggested that this observation could be a result of the polar nature of the ester penetrants, which could potentially lead to favorable polymer–ester interactions. It is now verified from the χ_{12} values listed in Tables 7 and 8 that the above suggestion is indeed consistent, i.e. the χ_{12} value for an ester is lower than that of a corresponding molar mass *n*-alkane indicative of more favorable polymer–penetrant interactions in the case of the ester. Thus, the trend observed in Fig. 2 for the lowest molecular weight esters where their behavior asymptotes that exhibited by the *n*-alkanes can also be understood by comparing their χ_{12} values to those of the remaining ester penetrants. Similarly, the lower E_d values for the esters larger than EP compared to the corresponding molar mass *n*-alkanes (in Fig. 3) can be explained by the lower χ_{12} values estimated for those esters. On the other hand, it is noted that the lowest molecular weight esters and alkanes coincide with each other and display a slope close to zero in Fig. 3. This is in spite of the lower χ_{12} values estimated for the esters, compared to the alkanes. All of this suggests that the transport properties of these lower molecular weight penetrants are not predominantly dictated by their chemical natures. Again, we are led to penetrants having a critical size beyond which chemical effects become significant.

So far, the χ values estimated in the present study have been used to describe the effects of the chemical nature of the penetrants on their transport behaviors. However, it should be mentioned that the explanations based on χ_{12} (inverse variation of D with χ) are based on the fact that the interactions between the polymer matrix and the two types of penetrants studied are found to be typical of poorer solvents. Very strong polymer–penetrant interactions such as in the case of systems comprising of aliphatic alcohols and polymers with hydrogen bonding ability [6] would result in low χ values and low diffusion coefficients, D. This behavior (direct variation of D with χ) forms the basis of many separation and chromatographic techniques.

3.3. Correlations

Below we summarize the above discussion that the diffusion properties of the *n*-alkanes and esters are influenced by a combination of two factors—*size* and *chemical nature* of the penetrants. It has been demonstrated that diffusivity increases with decreasing molecular size and increasing extent of specific interactions (lower χ). These results may be combined to yield a basic relationship, as follows:

$$D \propto 1/(\text{Mass} \times \chi_{12}) \tag{6}$$

Eq. (6) may be rewritten in terms of molar volume (V_m) as,

$$D \propto 1/(\text{Molar volume} \times \chi_{12}) \tag{7}$$

The above equations qualitatively describe the effects of *size and chemistry of the penetrants* on their transport process. According to expression (7), plots of log D versus $1/(\chi \times V_m)$ for the esters and *n*-alkanes at all test temperatures were made and are shown in Fig. 6. It is found that the data for the *n*-alkanes and esters (with the exception of IDP) at a given temperature may be represented by a single curve. However, Eqs. (6) and (7) above do not account for the temperature variation observed. In the present study, the activation energy of diffusion, E_d was used as the temperature-dependent parameter due to the fact that E_d describes the temperature dependence of the diffusion coefficient, D. E_d has also been shown [19,40–42] to be dependent upon the 'state' of a polymer (i.e. cohesive energy density, fractional free volume, etc.). The relationship between E_d and D was given by the Arrhenius equation such that Log(D) at a given temperature was related to the activation energy, E_d. Based on the above relationship, Eq. (7) may now be rewritten as:

$$E_d \propto \chi_{12} \times V_m \tag{8}$$

According to Eq. (8), a plot of E_d versus ($\chi \times V_m$) for all the

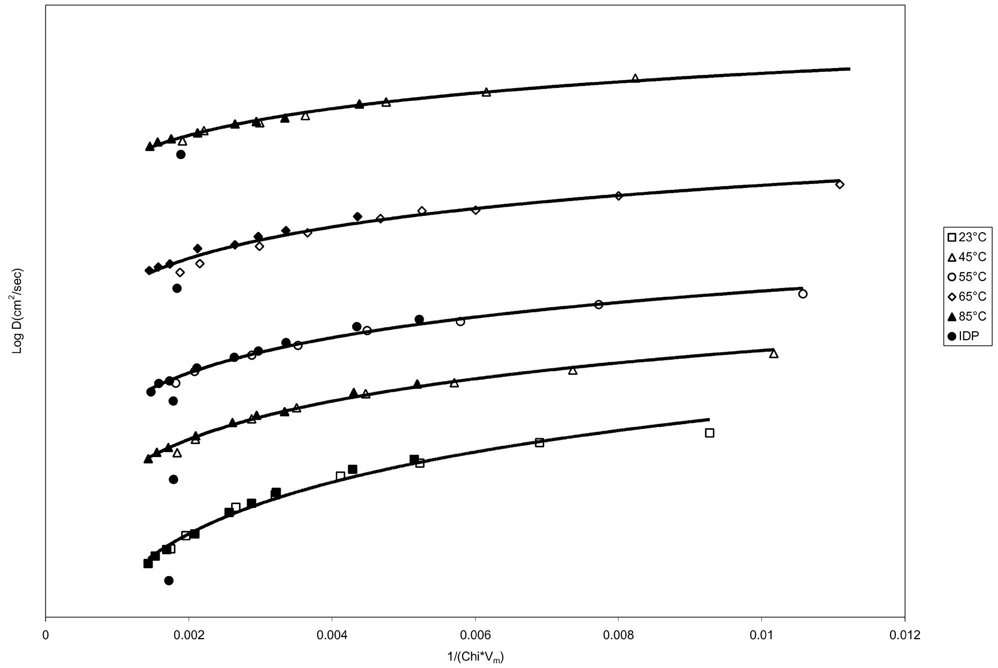

Fig. 6. Plot of log D (cm^2/s) versus $1/(\chi \times V_m)$ for esters and n-alkanes. Esters are designated with open symbols. Data have been shifted along the y-axis for the sake of clarity.

penetrants (except IDP) is shown in Fig. 7. It is seen that all the isotherms (a total of 85 data points) can be represented by a single first order exponential curve. This indicates that the incorporation of a parameter that accounts for temperature (such as E_d) markedly improves the description of the diffusion behaviors of the systems studied. Thus, a correlation has been developed that accurately describes the transport properties of polymer–penetrant systems (of the limited type studied) taking into account the size, shape and chemical nature of the penetrants at a given temperature. Presently, there is no such correlation available in the literature to the knowledge of the authors. The above correlation could lead to the concept of a multi-parameter model that accurately describes the transport properties of any polymer–penetrant system, similar to the ones studied.

4. Conclusions

The diffusion properties of a series of ester penetrants in a polyamide-based polymeric adhesive were investigated. The results obtained were compared with those from the

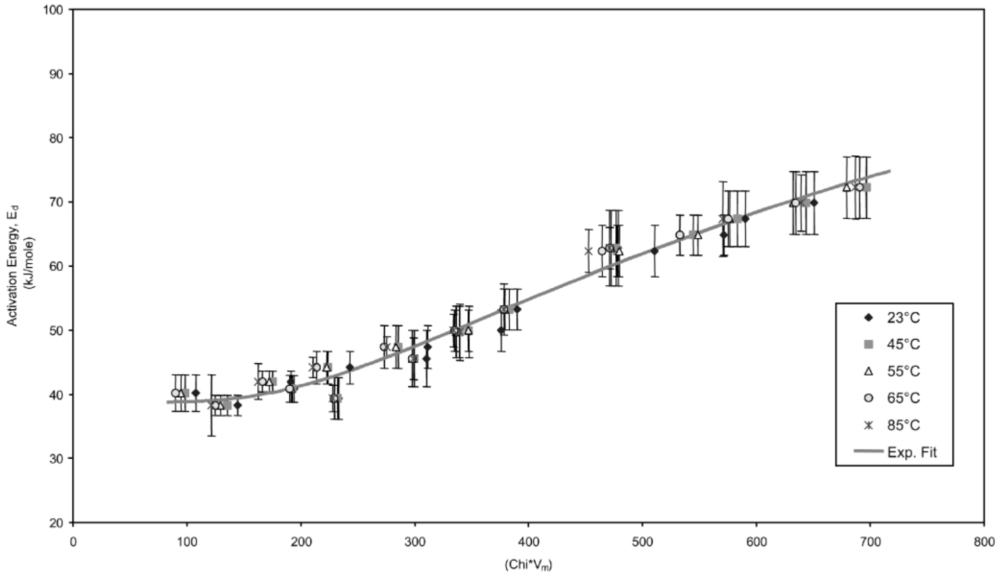

Fig. 7. Activation energy of diffusion, E_d (kJ/mol) for *n-alkanes* and *esters* versus $(\chi \times V_m)$. A first-order exponential has been shown since it can adequately describe the ‘plateau’ region at lower activation energies.

previous study on *n*-alkanes [1]. It was established that, as in the case of *n*-alkanes, the diffusion of esters is Fickian, follows first order kinetics and occurs via a Henry's law-type mechanism. However, unlike in the case of *n*-alkanes, gross deviations from the power law diffusion expression were obtained for the esters. This result implied that factors (such as penetrant shape and chemical nature) in addition to molar mass of the esters must influence their diffusion processes.

Information on the shape of the ester penetrants during their transport into the polymer matrix was obtained from a combination of molecular simulations and activation energy calculations. It was concluded that these penetrants (with the exception of IDP) like the *n*-alkanes, diffuse linearly along their long axes. Furthermore, the general shape of the penetrants was found to remain unchanged with increasing number of carbon units. From these results, it was inferred that the differences in the diffusion behaviors between *n*-alkanes and esters are not due to any noticeable differences in shapes of these penetrants (except IDP).

The chemical nature of the penetrants was studied by means of the Flory–Huggins interaction parameter, χ_{12}. The χ_{12} values for the esters were lower than those of the corresponding *n*-alkanes, suggesting favorable contributions to the polymer–ester interactions due to the polar ester functionality. Differences in the diffusion coefficients between the two types of penetrants were explained on the basis of their χ_{12} values.

The 'anomalous' behavior of IDP was attributed to the placement of the ester functionality in the middle of this molecule, thereby inducing a more spherical geometry and a larger diffusion cross-section. These factors, in addition to the increased shielding of the ester moiety in IDP, resulted in a diffusion mechanism that was different from that of the remaining ester penetrants.

Finally, correlations between (a) the diffusion parameters, D and E_d, (b) penetrant size (molar volume, V_m) and (c) chemical nature of the penetrant (χ) were established. These correlations account for both the size and chemical effects simultaneously, thereby providing a better description of the transport behaviors of the polymer–penetrant systems. The relationships were also successfully applied to both the penetrant series, due to the fact that their *shapes* and *mechanisms* were very similar.

Acknowledgements

The authors wish to thank Brett Kite for his assistance with the molecular simulations and members of the PolyPKem research group for valuable discussions. Additional thanks are also due to the Naval Surface Warfare Center, the Center for Adhesive and Sealant Science, the Adhesive and Sealant Council, and the National Science Foundation for the funding of this project.

Appendix A

It is known from the theories of rubber elasticity [38,39] that the modulus, E is related to the molecular weight between crosslinks, M_c (of the polymer network) by the following relationship.

$$E = \frac{3\rho_p RT}{M_c} \tag{9}$$

where ρ_p is the density of the polymer, R is the gas constant, and T is the temperature.

The derivation of this equation is based on the following assumptions:

1. That the polymer behaves as an ideal elastomer, and thereby the change in internal energy upon elongation is negligible,
2. That the polymer undergoes affine uniaxial deformation, and
3. The equation is derived in the limit of small strains.

In the present study, the equilibrium modulus, E for the polyamide-based polymer was determined from the stress relaxation experiment described in Section 2. This value was estimated to be 1.60 MPa based on the average of five specimens tested. The density of the polymer was experimentally determined to be equal to 1.0388 g/cm^3 at 150 °C. Substituting the above values in Eq. (9) yielded the M_c value for the polymer network, as being equal to 6887 ± 10%/mol of network chains. This value is of the same order of magnitude as the M_c values reported for many crosslinked systems such as natural rubber [43,44].

The molecular weight between crosslinks for the polymer, M_c determined from above was subsequently used in the evaluation of the Flory–Huggins interaction parameter, χ_{12}. This was done based on the FFR hypothesis, according to which,

$$M_c = \frac{-\rho_p V_m (c^{1/3} - c/2)}{\ln(1-c) + c + \chi_{12} c^2} \tag{10}$$

where c is the relative concentration of penetrant, V_m is the molar volume of solvent (cm^3/mol), and ρ_p is the density of polymer (g/cm^3).

The three main assumptions associated with this hypothesis are given below.

1. The change in free energy of a swollen system is the sum of changes in free energy due to polymer–penetrant mixing, and due to the elastic deformation of the polymer network.
2. The change in free energy due to polymer–penetrant mixing may be described by the lattice model of the Flory–Huggins theory, and
3. The elastic deformation of the polymer network may be described by an affine deformation.

The χ values for the polymer–penetrant systems in the present study at the different test temperatures were evaluated by substituting the values for M_c, ρ_p, c and V_m for a given system, in Eq. (10). The M_c, ρ_p and c values used were obtained experimentally, whereas the V_m values used were taken from the literature. (c values were obtained directly from the sorption data collected for the polymer–penetrant systems.)

References

[1] Kwan KS, Subramaniam C, Ward TC. Effect of penetrant size and shape on its transport through a thermoset adhesive. I. *n*-Alkanes. Accepted for publication in Polymer.
[2] Aminabhavi TM, Phayde HTS, Ortego JD, Stahl WM. J Appl Polym Sci 1997;63:1223–35.
[3] Aminabhavi TM, Munnoli RS. Can J Chem Engng 1994;72:1047–54.
[4] Koszinowski J. J Appl Polym Sci 1986;31:2711–20.
[5] Möller K, Gevert T. J Appl Polym Sci 1994;51:895–903.
[6] Aminabhavi TM, Khinnavar RS. Polymer 1993;34(5):1006–18.
[7] Shieh LY, Peppas NA. J Appl Polym Sci 1991;42:1579.
[8] Lucht LM, Peppas NA. J Appl Polym Sci 1987;33:1557.
[9] Harogoppad SB, Aminabhavi TM. Macromolecules 1991;24:2598.
[10] Balik CM. Macromolecules 1996;29:3025–9.
[11] Fujita H. Adv Polym Sci 1961;3:19.
[12] Fujita H, Kishimoto A. J Polym Sci 1958;25:547.
[13] von Meerwall E, Ferguson RD. J Appl Polym Sci 1979;23:3657.
[14] von Meerwall E, Skowronski D, Hariharan A. Macromolecules 1991; 24:2441.
[15] Storey RF, Mauritz KA, Cox BD. Macromolecules 1989;22:289–94.
[16] Chen SP, Edin JAD. Polym Engng Sci 1980;20(1):40–50.
[17] Kulkarni MG, Mashelkar RA. Polymer 1981;22:1665–72.
[18] Mauritz KA, Storey RF, George S. Macromolecules 1990;23(2): 441–50.
[19] Meares P. Polymers: structure and bulk properties. London: Van Nostrand; 1965.
[20] Gall TP, Lasky RC, Kramer EJ. Polymer 1990;31:1491–9.
[21] Koszinowski J. J Appl Polym Sci 1986;32:4765–86.
[22] Crank J, Park GS. Diffusion in polymers. London: Academic Press; 1968.
[23] Lawson AW. J Chem Phys 1960;19:131.
[24] Koros WJ. Barrier polymers and structures. Washington, DC: ACS; 1990.
[25] Hayer MJ, Park GS. Trans Faraday Soc 1955;51:1134.
[26] van Krevelen DW, Hoftyzer PJ. Properties of polymers, their estimation and correlation with chemical structure. Amsterdam: Elsevier; 1976.
[27] Harogoppad SB, Aminabhavi TM. Polymer 1991;32:5.
[28] Aminabhavi TM, Phayde HTS. Polymer 1986;36(5):1023–33.
[29] Aminabhavi TM, Phayde HTS. J Appl Polym Sci 1995;55:1335–52.
[30] Southern E, Thomas AG. J Polym Sci. (A) 1965;3:641.
[31] Southern E, Thomas AG. Trans Faraday Soc 1967;63:1913.
[32] Moisan JY. Eur Polym J 1981;17:857.
[33] Kwan KS. The role of penetrant structure on the transport and mechanical properties of a thermoset adhesive. PhD Dissertation, Virginia Tech, 1998
[34] Berens AR, Hopfenberg HB. J Membr Sci 1982;10:283.
[35] Roseveare WE, Powell RE, Eyring H. J Appl Phys 1941;12:669.
[36] Flory PJ. Principles of polymer chemistry. Ithaca, NY: Cornell University Press; 1953.
[37] Huggins ML. J Phys Chem 1942;46:151.
[38] Treloar LRG. The physics of rubber elasticity, 3rd ed. Oxford: Claredon Press; 1975.
[39] Wilkes GL. Private communication
[40] Duda JL, Vrentas JS, Ju ST, Liu HT. AIChE 1982;28(2):279–85.
[41] Pace RJ, Datyner A. J Polym Sci: Polym Phys Ed 1979;17:437–51.
[42] Ju ST, Duda JL, Vrentas JS. I EC Prod Res Dev 1981;20:330–5.
[43] McKenna GB, Flynn KM, Chen Y. Polym Commun 1988;29:272–5.
[44] McKenna GB, Flynn KM, Chen Y. Polymer 1990;31:1937–45.